Electrophysiological resting state brain network and episodic memory in healthy aging adults

Yuxuan Chen [a], Julia H. Tang [b], Lisa A. De Stefano [c,d], Michael J. Wenger [c,d], Lei Ding [b,e], Melissa A. Craft [f], Barbara W. Carlson [f], Han Yuan [b,e,*]

[a] *School of Electrical and Computer Engineering, University of Oklahoma, Norman, OK, United States*
[b] *Stephenson School of Biomedical Engineering, University of Oklahoma, Norman, OK, United States*
[c] *Department of Psychology, University of Oklahoma, Norman, OK, United States*
[d] *Graduate Program in Cellular and Behavioral Neurobiology, University of Oklahoma, Norman, OK, United States*
[e] *Institute for Biomedical Engineering, Science, and Technology, University of Oklahoma, Norman, OK, United States*
[f] *Fran and Earl Ziegler College of Nursing, University of Oklahoma Health Sciences Center, Oklahoma City, OK, United States*

ARTICLE INFO

ABSTRACT

Recent studies have emphasized the changes in large-scale brain networks related to healthy aging, with the ultimate purpose to aid in differentiating normal neurocognitive aging from neurodegenerative disorders that also arise with age. Emerging evidence from functional Magnetic Resonance Imaging (fMRI) indicates that connectivity patterns within specific brain networks, especially the Default Mode Network (DMN), distinguish those with Alzheimer's disease from healthy individuals. In addition, disruptive alterations in the large-scale brain systems that support high-level cognition are shown to accompany cognitive decline at the behavioral level, which is commonly observed in the aging populations, even in the absence of disease. Although fMRI is useful for assessing functional changes in brain networks, its high costs and limited accessibility discourage studies that need large populations. In this study, we investigated the aging-effect on large-scale networks of the human brain using high-density electroencephalography and electrophysiological source imaging, which is a less costly and more accessible alternative to fMRI. In particular, our study examined a group of healthy subjects in the age range from middle- to older-aged adults, which is an under-studied range in the literature. Employing a high-resolution computation model, our results revealed age associations in the connectivity pattern of DMN in a consistent manner with previous fMRI findings. Particularly, in combination with a standard battery of cognitive tests, our data showed that in the posterior cingulate / precuneus area of DMN higher brain connectivity was associated with lower performance on an episodic memory task. The findings demonstrate the feasibility of using electrophysiological imaging to characterize large-scale brain networks and suggest that changes in network connectivity are associated with normal aging.

1. Introduction

With advances in medical science and health care, the world is changing into a rapidly aging society (Beard et al., 2016). Neurodegenerative disorders, such as Alzheimer's disease (AD), have an enormous impact on the quality of life in millions of aging adults and bring a daunting financial burden to the society. Although several hypotheses are currently being pursued (Du et al., 2018; Edwards, 2019; Ittner and Götz, 2011; Karran et al., 2011), the lack of accurate clinical biomarkers for differentiating these disorders from normal aging has slowed the progress in establishing treatments that can be delivered early in the disease process (Crous-Bou et al., 2017; Cummings et al., 2016; McDade et al., 2021; Sperling et al., 2014).

Cognitive decline is commonly observed in aging even in the absence of diseases, affecting the functions of memory, execution, and attention (Ferreira and Busatto, 2013; Hedden and Gabrieli, 2004; Peters, 2006; Whalley et al., 2004). However, because the aging-related cognitive declines at non-pathological stage overlap with early symptom of cognitive deficit at preclinical or prodromal stage of AD (Ferreira and Busatto, 2013), early diagnosis of Alzheimer's disease remains difficult (Dubois et al., 2016; Fiandaca et al., 2014; Porsteinsson et al., 2021; Sperling et al., 2011). Therefore, in order to elucidate the pathogenesis of Alzheimer's disease, an augmenting attention has been raised to understanding normal aging (Cavedo et al., 2014; Ferreira and Busatto, 2013; Sperling et al., 2011).

One of the first critical steps is to devise screens capable of differentiating age-related neurocognitive declines from cognitive deficits seen at preclinical or prodromal stages of a neurodegenerative disorder (Cummings et al., 2016; Porsteinsson et al., 2021; Sperling et al., 2014). Well-designed experimental tasks and clinical batteries are widely deployed to detect the age-related differences in cognitive function (Donohue et al., 2014). In addition, cognitive deficits have been observed in fMRI studies of cognitive tasks tapping into wide-ranging domains of episodic memory (Tromp et al., 2015), working memory (Luo and Craik, 2008), attention (Madden, 1990), and executive task-switching (Cepeda et al., 2001). Nevertheless, the interpretation of task-based fMRI responses can be confounded by differences in task performance (Sheline and Raichle, 2013). Furthermore, task-based assessment of cognitive function may be biased by a number of factors that are bonded to the task design yet beyond the cognitive domains of interest (Grady, 2012; Healey et al., 2008). for example, older adults are recognized to be more susceptible to the effects of distracting interference during memory tasks (Grady, 2012; Healey et al., 2008), which suggest that a task-free strategy may be able to provide new insights.

Modern functional neuroimaging tools have dramatically shaped our knowledge of age-related changes in cognitive function. Recently, the use of task-free, resting-state functional connectivity imaging has resulted in rapidly growing literature on the nature and extent of network disruptions, which suggest the potential utility of functional connectivity as a biomarker for disease diagnosis, prognosis, and risks (Sheline and Raichle, 2013; Sperling, 2011). In particular, emerging evidence illustrates that brain connectivity within specific brain networks, especially the default mode network (DMN) (Buckner et al., 2005; Greicius et al., 2004), demonstrates patterns that characterize the trajectory of aging and distinguish healthy aging from Alzheimer's disease in both task-specific and task-free fMRI models (Eyler et al., 2019; Ibrahim et al., 2021).

DMN is composed of several regions which are known to be associated with various cognitive functioning (Buckner et al., 2008; Mevel et al., 2011): posterior cingulate cortex is associated with episodic memory encoding (Natu et al., 2019), the medial prefrontal cortex is linked with social cognition (Amodio and Frith, 2006), the medial temporal lobe is reported to contribute to episodic memory and episodic future thinking (Race et al., 2011), and the parietal cortex is associated with attention function (Behrmann et al., 2004). Notably, amyloid-beta plaques, one of Alzheimer's disease pathologies, are initially deposited in DMN subsets, such as posterior cingulate cortex and hippocampus (Buckner et al., 2005). Furthermore, disruptive alterations in the large-scale brain networks that support high-level cognition are shown to accompany cognitive decline at the behavior level, which is commonly observed in aging even in the absence of disease (Andrews-Hanna et al., 2007; Damoiseaux et al., 2007).

Although functional connectivity of DMN has been suggested as a biomarker for disease diagnosis and risks, fundamental limitations exist regarding the use of magnetic resonance imaging. The blood-oxygenation-level-dependent (BOLD) signal measured by fMRI is not a direct measurement of neuronal activities (Logothetis, 2008). Therefore, the interpretation of fMRI outcomes is confounded by non-neural cerebrovascular alterations associated with the disease (Chen, 2019; D'Esposito et al., 2003). Furthermore, fMRI imaging incurs high cost and has limited accessibility. However, understanding the early pathological process related to AD, especially in the preclinical stage, requires that a large population be studied. Power analysis for the prevention trials in Alzheimer's Disease usually yielded more than 1000 individuals are needed (Hsu and Marshall, 2017). Therefore, a more economic option for assessing the integrity of cognitive function via neuroimaging is demanded to enable more studies in large populations (Cavedo et al., 2014).

Electroencephalography (EEG), in contrast, measures neuronal activity of neural ensembles at hundreds of Hz, which is a significantly higher temporal resolution than fMRI. Recent studies from our group (Chen et al., 2021; Chen et al., 2019; Li et al., 2018; O'Keeffe et al., 2017; Yuan et al., 2016; Yuan et al., 2018; Yuan et al., 2014; Yuan et al., 2013; Yuan et al., 2012) and others (Custo et al., 2017; Liu et al., 2017) have demonstrated that network-level analysis of EEG signals reveals the functional connectivity of large-scale brain networks, including the default mode network. Our previous work has developed a method to reconstruct resting state brain networks by combining a high-resolution cortical model, electrophysiological source imaging, and analysis of the temporally independent EEG microstates (Yuan et al., 2016). Such EEG-derived DMNs have been validated with the fMRI resting state networks via simultaneous EEG and fMRI in human participants (Chen et al., 2021; Chen et al., 2019; Yuan et al., 2016; Yuan et al., 2018; Yuan et al., 2012). Furthermore, the large-scale networks reconstructed from EEG have been shown to detect the disease-modifying connectivity changes induced by a brain stimulation intervention (Chen et al., 2021; Chen et al., 2019; Li et al., 2018). Because EEG directly samples electrical neural activity, connectivity derived from EEG will not be subject to vascular coupling. Thus, the neural contribution to the fMRI derive network connectivity can be delineated separately from the vascular contribution using our EEG techniques.

In addition, as compared with fMRI, EEG provides supplementary features of economic efficiency, broad accessibility, and compatibility. Therefore, the current study aimed to examine age-related alterations in DMN in normal aging adults, towards the long-term goal of establishing an effective and economical biomarker to empower prevention studies. In our investigations, we tested the feasibility of reconstructing electrophysiological default mode network based on high-density EEG data recorded from the participants at an eyes-open resting state. Next, we compared the connectivity derived from the posterior cingulate/precuneus region of DMN with memory performance assessed by a standard cognitive battery. Our analysis tested the feasibility of creating a neuroimaging algorithm based on brain connectivity to assess the risk of pathological cognitive decline during normal aging, which may pave the way towards an objective, low-cost and accessible technology to detect cognitive impairment at an early phase.
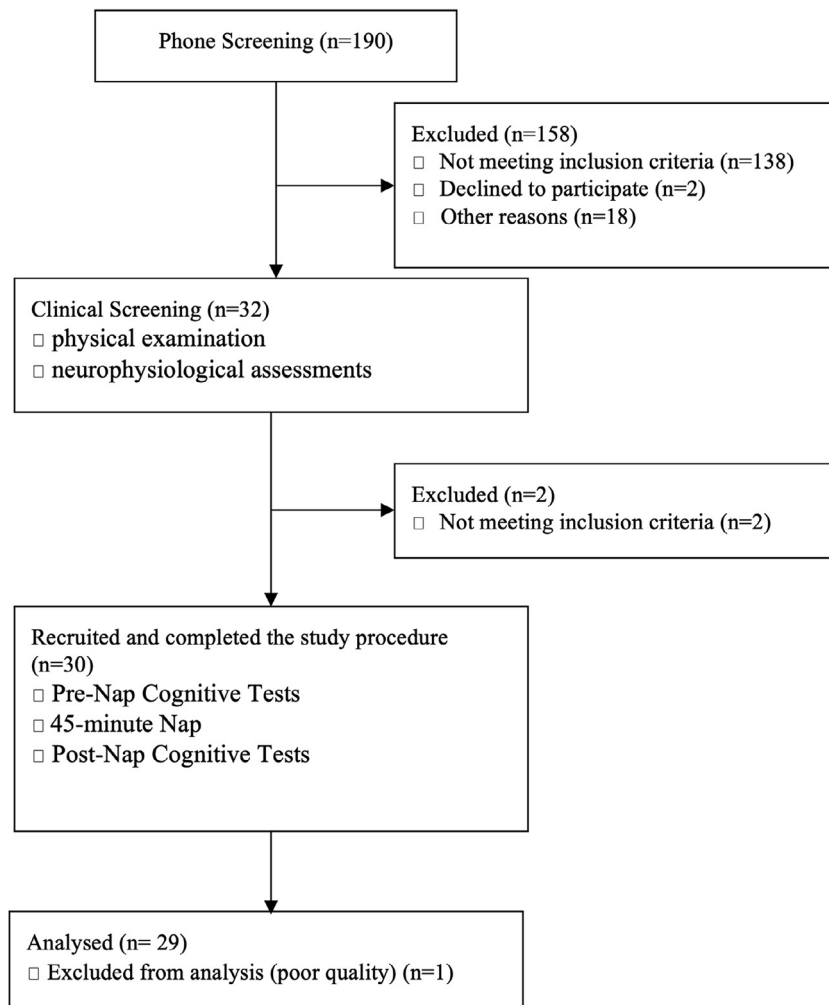
2. Methods and materials

2.1. Participants

The study protocol (shown in Fig. 1) was approved by the Institutional Review Board at the University of Oklahoma Health Sciences Center. Middle-aged and older adults were recruited from the local community. All were initially screened by telephone screen to excluded persons with significant neurological, neuropsychiatric, sleep, substance abuse, or cardiopulmonary disorders. After obtaining their written informed consent, they next underwent a physical examination (including blood pressure, temperature, pulse oximetry, heart rate) and neurophysiological assessments administered by a registered nurse to ensure that they were cognitively intact and with no significant chronic disease.

A total of 190 subjects were initially screened by telephone and 32 underwent clinical screening. Of the 30 who met our eligibility criteria, all of them were recruited and completed the study procedure, including a battery of cognitive tests and EEG recording. Data from one subject was removed due to the poor quality of the neuroimaging data, resulting a final sample size of twenty-nine subjects. The resulting groups consisted of 15 middle-aged adults (9 Female / 6 Male, 33.5 ± 4.9 years old, range 28 - 46 years old) and 14 older adults (12 Female / 2 Male, 55.3 ± 4.8 years old, range 48 - 62 years old).

2.2. Experimental paradigm

All subjects completed a standardized battery of clinical neurocognitive tests, which included both subscales of the immediate and delayed memory recall subscales of the Wechsler Logical Memory Test (Wechsler, 1987), the Symbol-Digit Modalities Test (Smith, 1982),

Fig. 1. Experimental procedure.

```
┌─────────────────────────────┐
│ Phone Screening (n=190)     │
└─────────────────────────────┘
           │
           │        ┌──────────────────────────────────────────┐
           ├───────▶│ Excluded (n=158)                         │
           │        │ □ Not meeting inclusion criteria (n=138) │
           │        │ □ Declined to participate (n=2)          │
           │        │ □ Other reasons (n=18)                   │
           │        └──────────────────────────────────────────┘
           ▼
┌─────────────────────────────┐
│ Clinical Screening (n=32)   │
│ □ physical examination      │
│ □ neurophysiological        │
│   assessments               │
└─────────────────────────────┘
           │
           │        ┌──────────────────────────────────────────┐
           ├───────▶│ Excluded (n=2)                           │
           │        │ □ Not meeting inclusion criteria (n=2)   │
           │        └──────────────────────────────────────────┘
           ▼
┌──────────────────────────────────────────┐
│ Recruited and completed the study        │
│ procedure (n=30)                         │
│ □ Pre-Nap Cognitive Tests                │
│ □ 45-minute Nap                          │
│ □ Post-Nap Cognitive Tests               │
└──────────────────────────────────────────┘
           │
           ▼
┌──────────────────────────────────────────┐
│ Analysed (n= 29)                         │
│ □ Excluded from analysis (poor quality)  │
│   (n=1)                                   │
└──────────────────────────────────────────┘
```

North American Reading Test (Uttl, 2002), Stroop Color-Word Test (Stroop, 1935), Clock-Drawing Test (CLOX 1) (Royall et al., 2000; Royall et al., 1998), and the Free and Cued Selective Reminding Test (Wenger et al., 2010). During the cognitive tests, the subjects sat still on a recliner in a quiet, well-lit experiment room and the recliner was put in the upright position. A voice recorder was put 30 cm in front of subjects and turned on to record all answers from subjects for future scoring. The experimenters sat alongside the subjects to instruct them to complete the memory task and recall sessions. The test battery was administered by a trained experimenter under a standard protocol to ensure both the consistency and accuracy of test administration and scoring. We employed the Immediate Recall score on the Logical Memory II from the Wechsler Memory Scale Fourth Edition (Wechsler, 1987) as the main score to assess the episodic memory performance, which has been well established to detect decline in prodromal dementia (Rabin et al., 2009) and detect early decline in the preclinical stages (Donohue et al., 2014).

2.3. Resting EEG data acquisition

Upon completing the cognitive test battery, a 64-channel whole-brain EEG cap based on the international 10–5 system was prepared in each participant. Conductive gel was added to all electrodes and the impedance was kept below 20 kΩ throughout the recording session. To ensure a secure fit, the front edge of the EEG cap was taped to the forehead and the distance between the edge of EEG cap and each subject's eyebrow was measured twice to verify the cap position at the beginning and the end of the recording.

Subjects were instructed to keep still and allowed to fall asleep during a 45 min recording of resting state, while subjects lied supine in an adjustable recliner with a neck-supporting pillow. While in position and before the resting recording started, impedance checking was performed to ensure that the impedance of all electrodes was below 20 kΩ, or conductive gel was re-applied if needed. The recording began and ended with bio-calibration, which were used to identify artifacts in the EEG recordings. The bio-calibration procedure was performed in a standard order of instructing subjects to (1) open and close their eyes, (2) blink, (3) perform lateral eye movements, (4) take deep breaths, (5) clench their teeth, and to (6) speak.

EEG data were recorded using a 64-channel ActiCHamp recording system (Brain Products, Munich, Germany), which consisted of two 32-channel amplifiers powered by a rechargeable battery unit. All the EEG datasets were digitized at a sampling rate of 500 Hz with a band-pass filtering of 0.1 Hz - 250 Hz. The onset and offset of the rest period were marked on the raw EEG.

2.4. EEG data processing

2.4.1. Selection of EEG recordings for connectivity analysis

The 45 minute recording was reviewed and manually scored into sleep stages by a certified expert B.W.C.), using standard scoring criteria by the American Academy of Sleep Medicine (AASM) (Berry et al., 2017). Briefly, EEG data were first segmented into epochs of 30-second length. Based on the frequency and amplitude of the signal, each segment was assigned of awake, non-rapid-eye-movement sleep (Stage 1
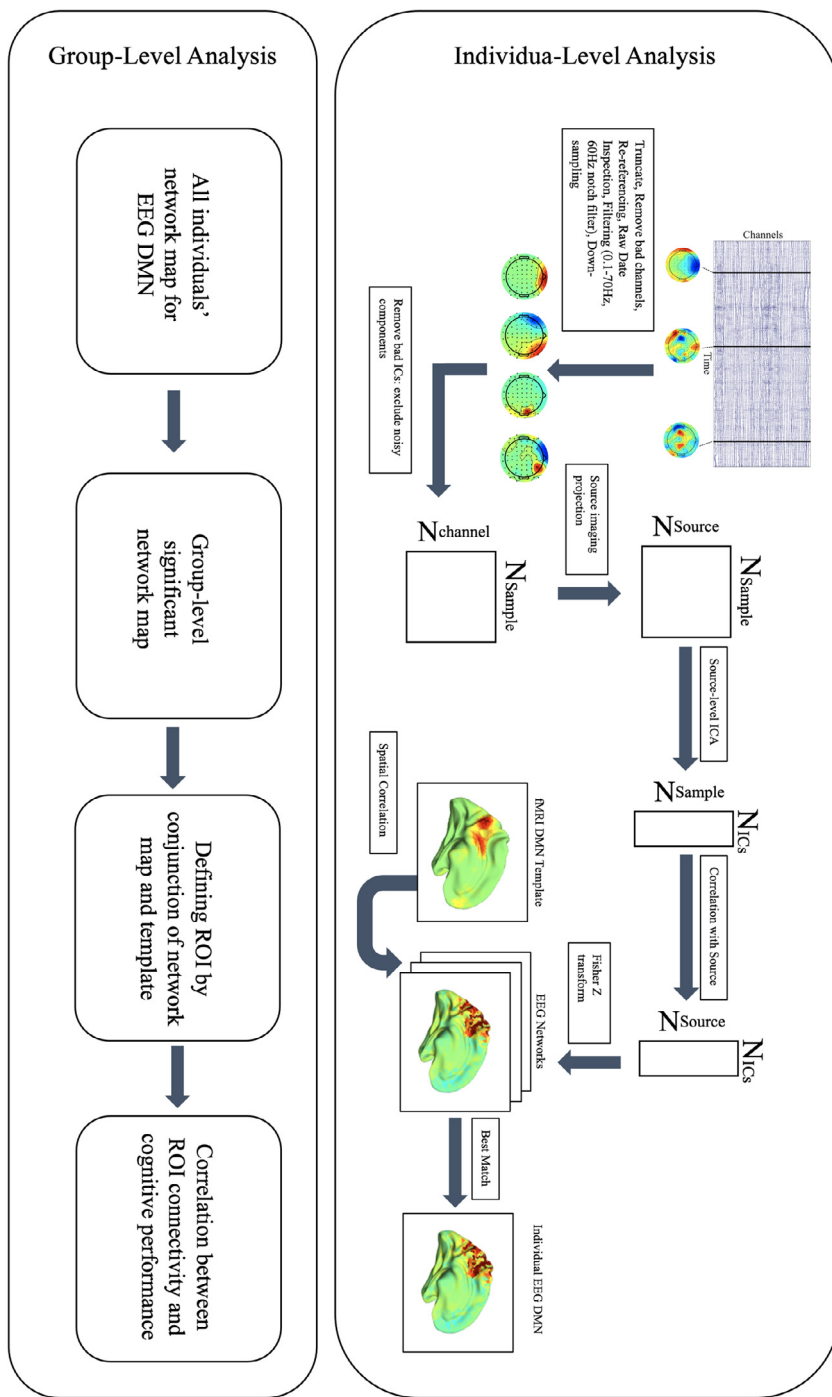
Fig. 2. The schematic diagram for data processing.

NREM, Stage 2 NREM), Slow Wave Sleep (Stage 3 NREM, Stage 4 NREM), or rapid-eye-movement sleep (REM). Only one participant remained awake for the entire 45 min. In the remaining 28 subjects, all had periods of wakefulness interspersed with sleep states. In order to differentiate awakening from sleep, we only selected segments of wakefulness before the onset of any sleep (regardless of where and how many times sleep states occurred in the rest of the recoding). We used multiple segments of wakefulness within an individual as test and re-test data, to verify the reliability of the EEG-derived networks. The sleep data were acquired for a separate purpose and thus not analyzed in the current study.

2.4.2. Preprocessing

Fig. 2 illustrates the analysis steps of our study. Preprocessing was performed with BrainVision Analyzer 2.0 (Brain Products, Munich, Germany) and MATLAB® 2015a (Mathworks Inc., Natick, Massachusetts, United States). Bad channels and segments were removed based on impedance checks and visual inspection. Based on the sleep staging, we truncated 3 minute resting-state recording of wakefulness before any sleep onset in each subject, as the default mode network has been shown to reach a stable pattern in a minimum of 2–3 min (Van Dijk et al., 2010). Five subjects fell asleep in less than 3 min and all recordings before sleep onset was kept. The resulting recording lengths for all subjects ranged from 35 s to 180 s (mean ± std = 169.1 ± 30.5 s). Next, the EEG

data was re-referenced to the common-average reference. The continuous EEG data in each channel were band-pass filtered from 0.1 Hz to 70 Hz with an extra notch filter at 60 Hz to eliminate powerline noise. Lastly, Independent Component Analysis (ICA) was applied to remove physiological artifacts, including vertical and horizontal ocular artifacts and muscle activity. These sources of artifact were further verified by comparing the recordings against the bio-calibration recordings.

2.4.3. Electrophysiological source imaging

Preprocessed EEG data were subjected to reconstruction of electrophysiological sources using a high-resolution cortical current source model. A template brain model in the MNI305 space was used as a common brain model for all subjects. The full segmentation and surface reconstruction of structural MRI was performed using the Freesurfer suite (https://surfer.nmr.mgh.harvard.edu/), resulting in a high-definition cortical layer and the brain, skull, and scalp boundary surfaces. These surfaces were then used to construct a three-compartment Boundary Element Method (BEM) model. Conductivity values were assigned to each compartment (Zhang et al., 2006). A standard profile of electrode positions in the 64-channel montage was digitized and co-registered to the fiducial points on the template brain. The high-density cortical layer mesh was down-sampled to 10,240 vertices per hemisphere and used as the source space. Each vertex corresponded to a dipole source oriented perpendicular to the surface. A lead-field matrix was then computed via a forward calculation using the cortical source space and the 3-layer BEM model. The calculation of source imaging returned the source matrix of N_{source} x N_{sample}, where the N_{source} is the number of dipole source points and N_{sample} is number of data points in time domain. The minimum norm method (Dale and Sereno, 1993; Hamalainen and Ilmoniemi, 1994) was used to solve the inverse problem.

2.4.4. Electrophysiological resting state network and connectivity

Based on the reconstructed source images, electrophysiological resting state networks were derived using the method established in Yuan et al. (2016). Considering that the participants enrolled in the study span across middle-age (28 - 46 years) and older age range (48 - 63 years), each individual's electrophysiological network was derived prior to group-level analysis, similar to the approach in Greicius et al. (2004). Specifically, source images of each individual at the down-sampled EEG microstates (Lehmann et al., 1987) were temporally concatenated. Afterwards, ICA was utilized to decompose the absolute values of source-level data into 25 independent components (ICs) for every subject, with each IC representing one distinctive brain network of the corresponding subject. The number of 25 ICs was chosen as it was shown to yield a reasonable representation of resting state networks in EEG that are also cross-modal validated in concurrent fMRI (Yuan et al., 2016; Chen et al., 2019; Chen et al., 2021). The time courses of brain networks were back-projected from the ICs, resulting in an activity matrix of N_{sample} x N_{IC}, where the N_{sample} is number of data points in time and N_{IC} is the number of source-level ICs. After calculating the source matrix and activity matrix, we further calculated the Pearson correlation coefficients between source matrix and activity matrix, resulting a matrix of N_{source} x N_{IC}. The connectivity value of brain networks was defined as the z-transformed correlation coefficient matrix.

For all 25 ICs, we depicted the source points on a standard brain model. Assuming each source-level IC represents one brain network, we focused on the DMN by searing for the best matched IC with a pre-defined DMN template. Specifically, the match was selected based on the spatial correlation calculated between the un-thresholded connectivity values of an EEG-derived network and the un-thresholded connectivity values of the template DMN derived from fMRI data in a separate group of healthy subjects (Yuan et al., 2016). One best match IC of highest spatial correlation coefficient was selected for every subject, which we referred as the individual-level DMN derived from EEG.For group-level analysis, individually derived network was smoothed before averaging to mitigate the anatomical discrepancy among individuals. Connectivity

values of the network matched to DMN were smoothed by employing a Gaussian filter with Full Width Half Maximum of 9 mm in FreeSurfer software. Then, the one sample *t*-test was used to determine the significance of DMN at the group level. Bonferroni correction was employed to control for multiple comparison problem.

2.4.5. Association between EEG network connectivity, memory and age

In order to assess the association between network connectivity and memory function, a region of interest (ROI) analysis was used. In brief, the group-level EEG DMN was obtained by performing a one-sample, two-sided *t* test on all subjects for every single dipole source point, as described above. In addition, the EEG network map was corrected by applying Bonferroni correction. The yielded EEG network was then further contained by intersection with a well-established Yeo template based on fMRI data from 1000 subjects (Yeo et al., 2011), also resulting in ROIs of EEG DMN for later analysis.

Episodic memory performance was quantified as the ratio of the number of first-time immediately recalled items from the Wechsler Logical Memory test over the total number of immediate recall items from that same test. The Immediate Logical Memory Subscale is a standardized test that generates three scores based on the recall of two short stories. The stories involve the Anna (story 1) and Joe (story 2), each of which are divided into 25 phrases. Each story is read aloud and immediately afterwards, the subject is asked to repeat as many details of the story as possible. The second story also serves as a distraction for the first, and so, after the second story about Joe, the subject is then asked to state as much as they can about the first story (Anna's Story). Due to its demonstrated sensitivity for detecting prodromal dementia (Donohue et al., 2014; Rabin et al., 2009), we calculate the ratio of summed scores from the first administration of Story 1 (Anna) over the total immediate memory score as a measure of episodic memory performance. In the Stroop task, subjects were given a sequence of 100 words and the correct percentage and total time length were recorded. We used a ratio of total length (sec.) and correct percentage (%) to assess the performance of Stroop (word only). The CLOX1 were scored by using a 15-column questionnaire (Royall et al., 1998) to assess how the subject draw the clock (the higher score, the better performance).

Then, the EEG network connectivity averaged within the ROI was compared to the corresponding logical memory score across all subjects. The partial correlation coefficient between connectivity values and memory scores was calculated. Furthermore, the network connectivity was compared with participants' age. The Pearson correlation coefficient between averaged connectivity values in the DMN ROI and ages was calculated.

As control analysis, we have investigated the visual network based on the reconstructed EEG source images, since functional connectivity of the visual network has been shown to be preserved in aging in the fMRI study (Andrews-Hanna et al., 2007). In a similar analysis strategy of the DMN, we have first identified the EEG visual network based on an fMRI template of the visual network. Individual EEG network of the highest spatial correlation with the template was selected. The EEG visual network of averaging individual maps was threshold at the $q < 0.05$ (one-sample, two-sided *t* test, with Bonferroni correction), resulting in a ROI for the EEG visual network. Then, individuals' EEG network connectivity within the ROI was extracted, averaged, and compared with the memory scores and ages across all subjects.

3. Results

Table 1 summarizes the demographic characteristics and performance on the cognitive battery. Subjects were recruited into two non-overlapping groups, i.e., a middle-aged group (range from 28 to 46 years old) and an older group (range from 48 to 63 years old); but the cognitive performance of the two age groups did not differ. The WMS Logical Memory score as the primary memory function performance did not

Table 1
Participant demographics and performance variables.

	Middle-Aged adults (n = 15)	Older adults (n = 14)
*Age, years	33.5 (4.9)	55.3 (4.8)
†Female / Male	9 / 6	13 / 2
MMSE, total score	29.4 (0.2)	29.3 (0.2)
WMS Logical Memory, immediate recall ratio	0.53 (0.03)	0.45 (0.03)
FCSRT, immediate recall ratio	0.49 (0.04)	0.43 (0.04)
Digit Symbol Modalities Test, total score	59.2 (2.3)	53.6 (2.1)
Stroop (word only), sec/correct%	52.6 (2.7)	48.6 (2.2)
CLOX1, total score	12.5 (0.5)	12.4 (0.3)

Mean and standard error (in parentheses) for participant demographics; MMSE: Mini-Mental State Examination; WMS: Wechsler Memory Scale; FCSRT: Free and Cued Selective Reminding Test; CLOX1:The executive clock drawing task. Gender difference was analyzed by using chi-square test
* shows significance difference between middle-age and older adult group, $p < 0.05$.
† shows significant difference between middle-age and older adult group, $p < 0.05$; the remaining variables were analyzed by using unpaired *t*-test.
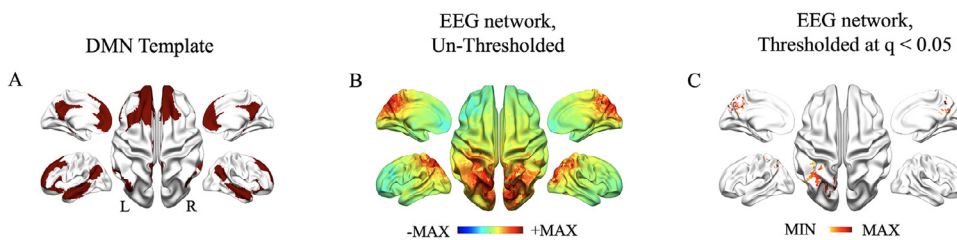

Fig. 3. Group-level average of the default mode network obtained from electrophysiological source images. (A) shows the template DMN parcellation from Yeo et al., 2011. (B) and (C) show maps of EEG DMN connectivity averaged across all subjects in (B) un-thresholded and (C) thresholded manner by one sample two-sided t test, corrected for multiple comparison.

differ significantly between the middle-aged and the older adults, although the older group was associated with marginally lower memory performance (t(27) = 1.88, p = 0.07). Supplemental Fig. 1 shows the WMS Logical Memory scores against individual ages in the middle-aged and older subjects. The two age groups overlap in the range of memory scores but follow distinctive trends in aging-related memory changes. Meanwhile, FCSRT score as the ratio of immediate recall did not differ between the two age groups (t(27) = 1.12, p = 0.27), while the FCSRT scores highly resembled the WMS Logical Memory scores (correlation coefficient = 0.42, p = 0.02). In addition, other cognitive scores did not differ between the age groups and are listed in Table 1. The digital symbol modality test as an assessment of working memory only marginally differed among two groups (t(27) = 1.81, p = 0.08).

The electrophysiological DMN obtained from all the subjects is shown in Fig. 3. The averaged and un-thresholded brain connectivity map is depicted in Fig. 3B. After thresholding and correcting for multiple comparison (Fig. 3C), the EEG DMN identified the posterior cingulate / precuneus area and the inferior parietal lobule, which are part of the key regions of DMN. Notably, the posterior region of EEG DMN presents stronger connectivity than the anterior regions. In addition, the un-thresholded maps of the EEG DMN showed that connectivity pattern extends to regions in the medial prefrontal cortex yet did not reach a group-level significance (Fig. 3B) . The maps of EEG DMN are consistent between the test and re-test data, as shown in Supplemental Fig. 2. The un-thresholded maps from test and re-test data yielded a spatial correlation coefficient of 0.84. The connectivity values from ROI were also consistent between the test and re-test data (r = 0.62, p < 0.001, Supplemental Fig. 2C). Furthermore, Supplemental Fig. 3 shows the separately reconstructed consistent maps of DMN from the sub-group of older adults and the sub-group of middle-aged adults, which yielded a spatial correlation coefficient of 0.66. However, the comparison of the connectivity patterns between the two age groups via an unpaired *t*-test with multiple comparison correction did not identify any regions with significant difference.

Because neither the cognitive performance nor the electrophysiological DMN differed significantly between the two age groups, our later analysis in seeking a relationship between the DMN connectivity, age
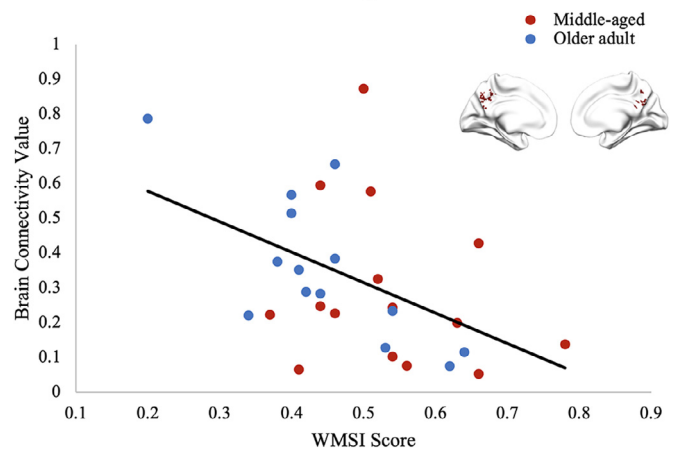

Fig. 4. Functional brain connectivity is correlated with memory performance across all subjects. The insert shows ROI regions defined from EEG DMN analysis. Brain connectivity values are calculated as the z-transformed correlation coefficients between individual's source time course and IC time course, averaged within the ROI. Each dot represents one individual's Brain connect. and the corresponding Wechsler Memory Scale Immediate Recall (WMSI) score. Red dots indicate middle-aged subjects and blue dots indicate older adults. Black trendline represents linear relationship between these two variables among all pooled subjects (r = -0.47, p = 0.01).

and memory performance has consolidated the two groups as one group. Fig. 4 shows the ROI analysis comparing individuals' brain connectivity values and their memory performance. The insert plot of Fig. 4 illustrates the ROI identified by a conjunction analysis of the group-level EEG DMN and the Yeo template, i.e. the conjunction of Fig. 3A and C. The ROI primarily includes posterior cingulate area, while part of it extends to the precuneus area. After extracting the connectivity values
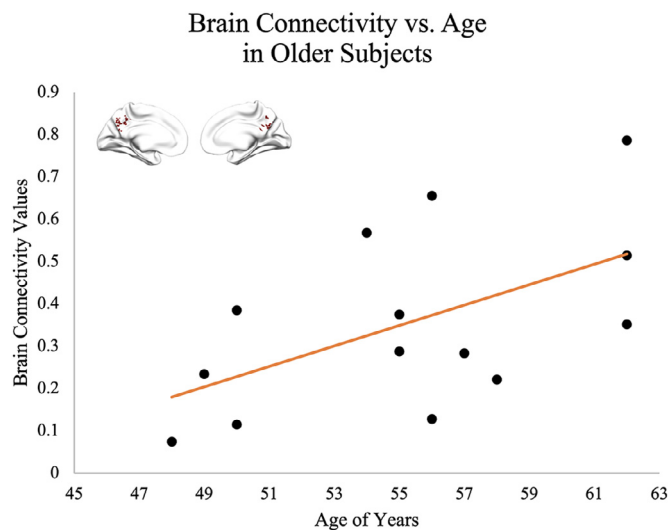
Fig. 5. Functional brain connectivity is correlated with age in older adults. The insert shows ROI regions defined from EEG DMN analysis. Brain connectivity values are calculated as the z-transformed correlation coefficients between individual's source matrix and activity matrix, averaged from ROI. Each black dot represents one individual's Brain connect. and the corresponding age of years. Orange trendline represents linear relationship between these two variables ($r = 0.55$, $p = 0.04$).

from the ROI, a significant negative correlation was identified between the connectivity averaged from ROI and the WMSI scores among all individuals ($r = -0.47$, $p = 0.01$). This finding indicated that subjects who had a better score of episodic immediate memory recall are associated with lower connectivity in the posterior DMN areas. In addition, considering that ages could also contribute to the association, we adopted a partial correlation analysis. After controlling the age factor, results still revealed a significant correlation between memory and network connectivity ($r = -0.42$, $p = 0.02$).

In addition, considering that the older adults follow a distinctive age-memory relationship than the middle-age subjects (as in Supplemental Fig. 1), our analysis explored the memory-connectivity relationship in the subset of older adults only, shown in Supplemental Fig. 4. Interestingly, the older adults show a consistent memory-connectivity trend in comparison with the middle-aged subjects, despite of a distinctive age-memory relationship. A similar and slightly stronger negative correlation was found in the subset of older adults ($r = -0.74$, $p = 0.003$), indicating that in the sub-group of older adults (ranging from 48 to 63 years old), better memory performance was associated with a lower connectivity in the ROI of posterior DMN.

Furthermore, we assessed the relationship between brain connectivity and the age (shown in Fig. 5). Interestingly, older aged subjects tend to show greater connectivity in the ROI of posterior DMN. Only in the sub-group of older adults, we found a significant correlation between the age and network connectivity in the ROI of posterior DMN ($r = 0.55$, $p = 0.04$, shown in Fig. 5). However, the association was not significant across all subjects (ages ranging from 28 to 63 years old, $r = 0.22$, $p > 0.1$), or not significant in the sub-group of middle-aged adults only ($r = -0.04$, $p > 0.1$).

As a control, we have performed the analysis on the EEG visual network. Following a similar strategy with the DMN, we have identified an EEG visual network by comparing with a template of fMRI visual network. The connectivity values from the ROI (by thresholding at $q < 0.05$) were extracted and compared with the memory performance. No significant linear association between the connectivity of the visual network and the WMSI scores was found among the individuals ($r = 0.16$, $p > 0.1$). The connectivity of the visual network was not correlated with the age, either ($r = -0.24$, $p > 0.1$). In none of the subgroups were any

significant correlation between the visual connectivity and WMSI or age (all $p > 0.1$).

4. Discussion

The current study utilized EEG to investigate the association between functional connectivity of resting state brain network and memory performance across normal healthy subjects in middle-aged and older age range. Our results demonstrated that the default mode network (DMN) can be reconstructed from the cortical source images derived from EEG at rest, including regions of the precuneus, posterior cingulate cortex, and the inferior parietal lobule. Furthermore, we found that network connectivity values within the ROI in posterior DMN were negatively correlated with episodic memory performance across healthy individuals ranging from middle ages to older ages. Meanwhile, in the sub-group of older adults, individuals' age was positively correlated with the connectivity from the same area in posterior DMN. The findings in this study reinforced our knowledge of the brain connectivity in DMN associated with advancing age. More importantly, brain connectivity assessed by this novel EEG-based neuroimaging technology is feasible to relate to a large number of clinical batteries to benchmark normal aging. This can potentially serve as an early biomarker of neurodegenerative disorders.

To date, DMN is one of the most important brain networks in fMRI studies on aging (for a review, see (Brier et al., 2014)). A number of studies have documented that resting-state functional connectivity in the DMN is sensitive to changes among groups of individuals with AD (Greicius et al., 2004; Wang et al., 2007; Zhang et al., 2009), prodromal AD including mild cognitive impairment (Bai et al., 2009; Petrella et al., 2011; Sorg et al., 2007), and healthy aging (Andrews-Hanna et al., 2007; Damoiseaux et al., 2007). Earlier studies of AD have consistently reported deterioration of connectivity in DMN, as compared with the healthy elders (Greicius et al., 2004; Wang et al., 2007; Zhang et al., 2009). Importantly, at the prodromal stage of AD (mild cognitive impairment), DMN connectivity was found to be abnormally impaired (Bai et al., 2008) and even associated with the risk of converting to AD-related dementia (Sorg et al., 2007). The metabolism hypothesis suggests that pathological changes in the DMN stimulate an activity-dependent or metabolism-dependent cascade that are spatially consistent with amyloid aggregations and tau pathology and, moreover, precedes and promotes the development of these AD pathology (Buckner et al., 2005), which is an important area being researched for developing intervention options. Therefore, identification of abnormal disruption of human brain networks, including DMN and other cognitively relevant network, appears to be essential in characterizing normal aging. Such characterization is also critical for identification of early pre-clinical stages in AD and early prevention in conjunction with pharmaceutical intervention (Sperling, 2011).

Recently, an increasing number of studies have extended the investigation of DMN in normal healthy individuals across the age range from elders to younger adults, with the purpose that establishing a normal aging trajectory will aid in the early diagnostics of preclinical stages in AD (Andrews-Hanna et al., 2007; Damoiseaux et al., 2007; Ferreira et al., 2016; Sambataro et al., 2010). Overall, the aging trajectory of brain connectivity do not follow a monotonic decrease, which our data on the DMN connectivity also confirms. Although it is well recognized that the connectivity within DMN was lower in the advanced elderly population (65+ years) as compared to the young adult population (Andrews-Hanna et al., 2007; Damoiseaux et al., 2008), literature on the aging adults of less than 65 years have controversial reports on the age association in DMN connectivity - whether age increase or decrease - that depends on the age range of study participants as well as the methodology of analyzing the connectivity (Andrews-Hanna et al., 2007; Ball et al., 2017; Damoiseaux et al., 2007; Jockwitz et al., 2017; Jones et al., 2011; Zonneveld et al., 2019). Although the age range that our study has examined was not available in the Andrews-Hann et al. study (2007), our finding on the age-connectivity relationship is supported with the fMRI

findings in the overlapping age range (Ball et al., 2017; Zonneveld et al., 2019). Meanwhile, the methodology of identifying DMN, especially sub-networks of DMN, has complicated the reported findings. Several of aforementioned studies (Ball et al., 2017; Damoiseaux et al., 2007; Jones et al., 2011; Zonneveld et al., 2019) applied a data-driven approach to parcellate the whole brain into units of functional networks prior to compare brain connectivity with the ages. Instead of masking out the whole DMN, the well-known resting-state network was further delineated into the anterior DMN and posterior DMN. Even though they are two subsets of DMN, each sub-network features age-related changes in both posterior and anterior areas of DMN, sometime even an opposite effect (Jones et al., 2011). Several studies agreed on negative association regarding anterior DMN - lower connectivity with older age (Damoiseaux et al., 2007; Zonneveld et al., 2019). In the meanwhile, our finding of the age increase in the older adults (45–64 years) is supported by a similar age increase in the posterior DMN (Ball et al., 2017; Zonneveld et al., 2019). Noteworthy, a population-based study of 711 older adults (55–85 years of age) found no age-related changes in the DMN (Jockwitz et al., 2017). Importantly, in that study, the DMN was not divided into its anterior and posterior subsystems, indicating the potential relevance of investigating DMN at different scales of functional organization.

To our knowledge, our study provides the *first* electrophysioglocal evidence of aging effect on a large-scale brain network - the default mode network. Our findings (in Fig. 5) revealed the age-related increase in the posterior cingulate cortex, which supports the positive association in posterior DMN identified in previous studies of overlapping age range (Ball et al., 2017; Zonneveld et al., 2019). Also, the areas of age-associated increase revealed in our restuls included additional precueus area that extends to the margin with cunes, which is in part consistent with the finding by Jones et al. (2011) that an age-associated increase in the edge of cunes as part of the posterior DMN. However, Jones et al. (2011) also reported an adjacent yet predominant age-associated decrease in posterior cingulate cortex as part of the posterior DMN, which was not observed in our study. The reason of not seeing a age-related decrease could be due to the different age-range examined in our study, or due to a discrepency on the vascular contributions.

In comparing our results with the abovementioned studies, it is import to note that our study employed electrophysiological measurements to investigate the age-related effect in DMN, while the functional MRI studies are based on hemodynamic measurements (e.g. blood-oxygenation-level-dependent contrast), which are secondary signals that involves blood flow and oxygenation in brain tissues (Logothetis et al. 2008). Thus, the age-connectivity relationship as documented by fMRI studies could be attriued to three possible origins - the neurons, the vasculature, or the neurovascular coupling unit. The neurovascular coupling is known to be suseptible to aging (D'Esposito et al., 2003; Ferreira and Busatto, 2013; Liu, 2013) and regional, aging-specific differences are reflected in vasculature (Chen, 2019; Sweeney et al., 2018), all of which could contribute to the observed aging phenomenon in fMRI. Nonetheless, our findings based on electrophysiolgocial recordings provide direct evidence supporting the age-related changes in neuronal activities, especially at the network-level connectivtiy. Despite the different modalities used, our EEG study and a number of fMRI studies have employed a similar data-driven approach to identify resting state brain networks and the age-association in the network connectivity. The template that our study employed to identify the DMN should be considered as posterior DMN rather than anteriror DMN, because of the predominant coposition in the posterior cingulate cortex and precuneus, which agrees with the posterior DMN examined in Zonneveld et al. (2019) and Jones et al. (2011). As direct measurement of neural activity, our findings from EEG provide the evidence to cross-validate some of fMRI findings regarding the functional connectivity associated with advancing age.

In addition to the age association, our findings stressed the functional role of PCC. Memory function has been well described as a dis-

tributed process (Mesulam, 1990), and the brain substrates and modifiers of this process are highly variable, particularly in a cognitive aging context (Braskie et al., 2010; Head et al., 2008; Raz and Rodrigue, 2006; Verhaeghen et al., 1993). As part of a well-connected neural network underlying the memory function, PCC is involved in episodic memory encoding (Natu et al., 2019) and also is one of the most vulnerable area prone to amyloid-beta deposition (Buckner et al., 2008; Ferreira and Busatto, 2013). By defining the ROI mainly in PCC (Fig. 4), our results have shown a significant negative correlation with memory performance on the averaged brain connectivity, which is exactly reversed to the age-association seen in our cohort especially in the older adults. Notably, the memory-connectivity association (Fig. 4) was robust in the entire participant ensemble across middle-aged and older adults, although the memory performance did not differ significantly between two age sub-groups, even in opposite trends (Supplemental Fig. 1). Higher performance of immediate memory recall was associated with lower functional connectivity in the posterior DMN, significantly seen in the entire group (28 to 63 years old, r = -0.47 and p = 0.01) as well as in the sub-group of older adults (48 to 63 years old, r = -0.74 and p = 0.003). Previous study has suggested that different subsets of DMN were not simultaneously activated (Sestieri et al., 2011). They found the PCC/precuneus were significantly activated during memory retrieval, whereas the anterior DMN is deactivated, which points out that the functional association in posterior DMN should be delineated separately from the anterior DMN. Nonetheless, the key regions of DMN at task-less, resting state exhibit fluctuations that are coherently synchronized, which are characterized as resting state functional connectivity. Furthermore, the intrinsic connectivity of resting state brain networks, especially DMN, have been found to be associated with memory performance. The association of a steady-state functional connectivity in the default mode network with memory function is observed in both cognitively intact individuals (Newton et al., 2011; Wang et al., 2010) and diseased populations (Bai et al., 2009; Mormino et al., 2011). Notably, in these studies the resting state scans are acquired either subsequently or prior to the function-probing tasks. It has been suggested that such changes in network-level connectivity observed in the normal aging stage occur as a result of insult brought by the amyloid accumulation happening at the preclinical AD-Stage (Sheline and Raichle, 2013). Thus, abnormalities in resting state functional connectivity can be detected in companion with or even before structural damage is manifested as atrophy and furthermore before cognitive decline produces clinical deterioration. In line with the model of progression events (Sheline and Raichle, 2013), our study demonstrated that reconstructed EEG source brain connectivity can reliably reveal aging effect in cognitively normal adults. The finding that the greater brain connectivity is associate with worse episodic memory performance in normal older adults suggests a compensatory mechanism in these overall cognitively normal individuals (Bishop et al., 2010), which is similarly observed in individuals at preclinical stage (Filippini et al., 2009) or at amnestic mild cognitive impairment stage (Qi et al., 2010). Through examining the DMN connectivity at different stages along the AD continuum: without cognitive impairment, SCD, early-stage MCI, late-stage MCI and AD, recent data from the Alzheimer's Disease Neuroimaging Initiative suggest that the network failure associated with AD starts in the posterior components of the DMN before amyloid plaques can be identified by PET imaging and spread to other brain areas through network hubs (Jones et al., 2016; Sintini et al., 2021). Our findings again stressed the importance of PCC as part of DMN in future aging studies in order to establish a full trajectory spanning normal aging, preclinical and clinical stages (Yu et al., 2021).

Nonetheless, several limitations in our study should be acknowledged. First, our sample size is relatively small (a total of 29 subjects), compared to many recent studies that recruited hundreds of subjects to investigate the aging association in brain networks (Jones et al., 2011; Zonneveld et al. 2019). Nonetheless, our sample size is comparable to early fMRI studies who explored DMN in the aging process

(Greicius et al., 2004; Damoiseaux et al., 2007). Given a small sample recruited in our study, the education history of subjects ranged from high school to postgraduate degrees, although all participants have completed education of high-school or above and the two subgroups did not differ in the years of education. Furthermore, the EEG DMN identified in our study showed weak connectivity in medial prefrontal cortex as compared with the template DMN from fMRI. It is possible that different sensitivity and specificity of EEG and fMRI modalities could contribute to the spatial difference (Nunez and Ramesh, 2006). In addition, it is also possible that the nonlinear dynamics of the electrophysioglocal activities captured in a high temporal resolution (Hipp et al., 2012; de Pasquale et al., 2010; de Pasquale et al., 2012), especially between long-distanced regions, might have contributed to the spatial difference. Nonetheless, our analysis of several independent concurrent EEG and fMRI datasets has confirmed that such an EEG DMN with posterior dominance has activities that are temporally correlated with the fMRI activities in long-ranged DMN areas including medial frontal cortex and inferior parietal lobules (Chen et al., 2021; Chen et al., 2019; Yuan et al., 2016).

In summary, we used EEG resting state recordings to characterize the functional connectivity alteration during normal aging process. Our findings indicate that the reconstructed EEG data at source level was capable of capturing the neural connectivity in a part of default mode network reliably. More importantly, the reconstructed cortical level connectivity was correlated to ages and memory performance assessed by clinical cognitive batteries. Our results indicate that EEG-derived network imaging can be used in monitoring network-level functional connectivity and detecting cognitive function alteration in healthy adults during normal aging process. This pilot evidence further suggests the use of EEG-network based neuroimaging in the study of aging and Alzheimer's disease related dementia.

Declaration of Competing Interest

None of authors disclose any potential conflict of interest.

Credit authorship contribution statement

Yuxuan Chen: Investigation, Formal analysis, Methodology, Writing – original draft, Writing – review & editing. **Julia H. Tang:** Investigation, Formal analysis, Writing – original draft. **Lisa A. De Stefano:** Investigation, Formal analysis, Writing – original draft. **Michael J. Wenger:** Conceptualization, Methodology, Funding acquisition, Supervision, Writing – original draft. **Lei Ding:** Conceptualization, Methodology, Funding acquisition, Writing – original draft. **Melissa A. Craft:** Investigation, Formal analysis, Writing – original draft. **Barbara W. Carlson:** Conceptualization, Formal analysis, Methodology, Funding acquisition, Writing – original draft, Supervision.

Acknowledgments

Data and code availability

Data used in this study are not publicly available due to research data sharing restrictions from the IRB, but are available from the corresponding author through a data use agreement. Software source code supporting the conclusions of this article is Matlab-based, and is available from the corresponding author upon reasonable request.

Supplementary materials

Supplementary material associated with this article can be found, in the online version, at doi:10.1016/j.neuroimage.2022.118926.

References

Amodio, D.M., Frith, C.D., 2006. Meeting of minds–The medial frontal cortex and social cognition. Nat. Rev. Neurosci. 7, 268–277.

Andrews-Hanna, J.R., Snyder, A.Z., Vincent, J.L., Lustig, C., Head, D., Raichle, M.E., Buckner, R.L., 2007. Disruption of large-scale brain systems in advanced aging. Neuron 56, 924–935.

Bai, F., Watson, D.R., Yu, H., Shi, Y., Yuan, Y., Zhang, Z., 2009. Abnormal resting-state functional connectivity of posterior cingulate cortex in amnestic type mild cognitive impairment. Brain Res. 1302, 167–174.

Bai, F., Zhang, Z., Yu, H., Shi, Y., Yuan, Y., Zhu, W., Zhang, X., Qian, Y., 2008. Default-mode network activity distinguishes amnestic type mild cognitive impairment from healthy aging–A combined structural and resting-state functional MRI study. Neurosci. Lett. 438, 111–115.

Ball, G., Beare, R., Seal, M.L., 2017. Network component analysis reveals developmental trajectories of structural connectivity and specific alterations in autism spectrum disorder. Hum. Brain Mapp. 38, 4169–4184.

Beard, J.R., Officer, A., de Carvalho, I.A., Sadana, R., Pot, A.M., Michel, J.-P., Lloyd-Sherlock, P., Epping-Jordan, J.E., Peeters, G.M.E.E.G., Mahanani, W.R., Thiyagarajan, J.A., Chatterji, S., 2016. The World report on ageing and health–A policy framework for healthy ageing. Lancet (London, England) 387, 2145–2154.

Behrmann, M., Geng, J.J., Shomstein, S., 2004. Parietal cortex and attention. Curr. Opin. Neurobiol. 14, 212–217.

Berry, R.B., Brooks, R., Gamaldo, C., Harding, S.M., Lloyd, R.M., Quan, S.F., Troester, M.T., Vaughn, B.V., 2017. AASM scoring manual updates for 2017 (Version 2.4). J. Clin. Sleep Med. 13, 665–666.

Bishop, N.A., Lu, T., Yankner, B.A., 2010. Neural mechanisms of ageing and cognitive decline. Nature 464, 529–535.

Braskie, M.N., Small, G.W., Bookheimer, S.Y., 2010. Vascular health risks and fMRI activation during a memory task in older adults. Neurobiol. Aging 31, 1532–1542.

Brier, M.R., Thomas, J.B., Ances, B.M., 2014. Network dysfunction in Alzheimer's disease–Refining the disconnection hypothesis. Brain Connectivity 4, 299–311.

Buckner, R.L., Andrews-Hanna, J.R., Schacter, D.L., 2008. The brain's default network–Anatomy, function, and relevance to disease. Ann. N. Y. Acad. Sci. 1124, 1–38.

Buckner, R.L., Snyder, A.Z., Shannon, B.J., LaRossa, G., Sachs, R., Fotenos, A.F., Sheline, Y.I., Klunk, W.E., Mathis, C.A., Morris, J.C., Mintun, M.A., 2005. Molecular, structural, and functional characterization of Alzheimer's disease–Evidence for a relationship between default activity, amyloid, and memory. J. Neurosci. 25, 7709–7717.

Cavedo, E., Lista, S., Khachaturian, Z., Aisen, P., Amouyel, P., Herholz, K., Jack Jr., C.R., Sperling, R., Cummings, J., Blennow, K., O'Bryant, S., Frisoni, G.B., Khachaturian, A., Kivipelto, M., Klunk, W., Broich, K., Andrieu, S., de Schotten, M.T., Mangin, J.F., Lammertsma, A.A., Johnson, K., Teipel, S., Drzezga, A., Bokde, A., Colliot, O., Bakardjian, H., Zetterberg, H., Dubois, B., Vellas, B., Schneider, L.S., Hampel, H., 2014. The road ahead to cure Alzheimer's disease–Development of biological markers and neuroimaging methods for prevention trials across all stages and target populations. J. Prev. Alzheimers Dis. 1, 181–202.

Cepeda, N.J., Kramer, A.F., Gonzalez de Sather, J.C.M., 2001. Changes in executive control across the life span–Examination of task-switching performance. Dev. Psychol. 37, 715–730.

Chen, J.J., 2019. Functional MRI of brain physiology in aging and neurodegenerative diseases. Neuroimage 187, 209–225.

Chen, Y., Cha, Y.H., Gleghorn, D., Doudican, B.C., Shou, G., Ding, L., Yuan, H., 2021. Brain network effects by continuous theta burst stimulation in Mal de Débarquement Syndrome–Simultaneous EEG and fMRI study. J. Neural Eng. 18 (6). doi:10.1088/1741-2552/ac314b.

Chen, Y., Cha, Y.H., Li, C., Shou, G., Gleghorn, D., Ding, L., Yuan, H., 2019. Multimodal imaging of repetitive transcranial magnetic stimulation effect on brain network–A combined electroencephalogram and functional magnetic resonance imaging study. Brain Connect. 9, 311–321.

Crous-Bou, M., Minguillón, C., Gramunt, N., Molinuevo, J.L., 2017. Alzheimer's disease prevention–From risk factors to early intervention. Alzheimer's Res. Ther. 9, 71.

Cummings, J., Aisen, P.S., DuBois, B., Frölich, L., Jack, C.R., Jones, R.W., Morris, J.C., Raskin, J., Dowsett, S.A., Scheltens, P., 2016. Drug development in Alzheimer's disease–The path to 2025. Alzheimer's Res. Ther. 8, 39.

Custo, A., Van De Ville, D., Wells, W.M., Tomescu, M.I., Brunet, D., Michel, C.M., 2017. Electroencephalographic resting-state networks–Source localization of microstates. Brain connect. 7, 671–682.

Damoiseaux, JS, Beckmann, CF, Arigita, EJ, Barkhof, F, Scheltens, P, Stam, CJ, Smith, SM, Rombouts, SA, 2008 Aug. Reduced resting-state brain activity in the "default network" in normal aging. Cereb Cortex 18 (8), 1856–1864. doi:10.1093/cercor/bhm207.

D'Esposito, M., Deouell, L.Y., Gazzaley, A., 2003. Alterations in the BOLD fMRI signal with ageing and disease–A challenge for neuroimaging. Nat. Rev. Neurosci. 4, 863–872.

Dale, A.M., Sereno, M.I., 1993. Improved Localizadon of cortical activity by combining EEG and MEG with MRI cortical surface reconstruction–A linear approach. J. Cogn. Neurosci. 5, 162–176.

Damoiseaux, J.S., Beckmann, C.F., Arigita, E.J.S., Barkhof, F., Scheltens, P., Stam, C.J., Smith, S.M., Rombouts, S.A.R.B., 2007. Reduced resting-state brain activity in the "default network" in normal aging. Cereb. Cortex 18, 1856–1864.

Donohue, M.C., Sperling, R.A., Salmon, D.P., Rentz, D.M., Raman, R., Thomas, R.G., Weiner, M., Aisen, P.S., 2014. The preclinical Alzheimer's cognitive composite–Measuring amyloid-related decline. JAMA Neurol. 71, 961–970.

Du, X., Wang, X., Geng, M., 2018. Alzheimer's disease hypothesis and related therapies. Transl. Neurodegeneration 7, 2.

Dubois, B., Hampel, H., Feldman, H.H., Scheltens, P., Aisen, P., Andrieu, S., Bakardjian, H., Benali, H., Bertram, L., Blennow, K., Broich, K., Cavedo, E., Crutch, S., Dartigues, J.F., Duyckaerts, C., Epelbaum, S., Frisoni, G.B., Gauthier, S., Genthon, R., Gouw, A.A., Habert, M.O., Holtzman, D.M., Kivipelto, M., Lista, S., Molinuevo, J.L., O'Bryant, S.E., Rabinovici, G.D., Rowe, C., Salloway, S., Schneider, L.S., Sperling, R., Teichmann, M., Carrillo, M.C., Cummings, J., Jack Jr., C.R., 2016. Preclinical Alzheimer's disease–Definition, natural history, and diagnostic criteria. Alzheimers Dement. 12, 292–323.

Edwards, F.A., 2019. A unifying hypothesis for Alzheimer's Disease–From plaques to neurodegeneration. Trends Neurosci. 42, 310–322.

Eyler, L.T., Elman, J.A., Hatton, S.N., Gough, S., Mischel, A.K., Hagler, D.J., Franz, C.E., Docherty, A., Fennema-Notestine, C., Gillespie, N., Gustavson, D., Lyons, M.J., Neale, M.C., Panizzon, M.S., Dale, A.M., Kremen, W.S., 2019. Resting state abnormalities of the default mode network in mild cognitive impairment–A systematic review and meta-analysis. J. Alzheimers Dis. 70, 107–120.

Ferreira, L.K., Busatto, G.F., 2013. Resting-state functional connectivity in normal brain aging. Neurosci. Biobehav. Rev. 37, 384–400.

Ferreira, L.K., Regina, A.C.B., Kovacevic, N., Martin, M.d.G.M., Santos, P.P., Carneiro, C.d.G., Kerr, D.S., Amaro Jr, E., McIntosh, A.R., Busatto, G.F., 2016. Aging effects on whole-brain functional connectivity in adults free of cognitive and psychiatric disorders. Cereb. Cortex 26, 3851–3865.

Fiandaca, M.S., Mapstone, M.E., Cheema, A.K., Federoff, H.J., 2014. The critical need for defining preclinical biomarkers in Alzheimer's disease. Alzheimers Dement. 10, S196–S212.

Filippini, N., MacIntosh, B.J., Hough, M.G., Goodwin, G.M., Frisoni, G.B., Smith, S.M., Matthews, P.M., Beckmann, C.F., Mackay, C.E., 2009. Distinct patterns of brain activity in young carriers of the APOE-epsilon4 allele. Proc. Natl. Acad. Sci. U. S. A. 106, 7209–7214.

Grady, C., 2012. The cognitive neuroscience of ageing. Nat. Rev. Neurosci. 13, 491–505.

Greicius, M.D., Srivastava, G., Reiss, A.L., Menon, V., 2004. Default-mode network activity distinguishes Alzheimer's disease from healthy aging–Evidence from functional MRI. Proc. Natl. Acad. Sci. U. S. A. 101, 4637–4642.

Hamalainen, M.S., Ilmoniemi, R.J., 1994. Interpreting magnetic fields of the brain–Minimum norm estimates. Med. Biol. Eng. Comput. 32, 35–42.

Head, D., Rodrigue, K.M., Kennedy, K.M., Raz, N., 2008. Neuroanatomical and cognitive mediators of age-related differences in episodic memory. Neuropsychology 22, 491–507.

Healey, M.K., Campbell, K.L., Hasher, L., 2008. Chapter 22 Cognitive aging and increased distractibility–Costs and potential benefits. In: Sossin, W.S., Lacaille, J.-C., Castellucci, V.F., Belleville, S. (Eds.), Progress in Brain Research. Elsevier, pp. 353–363.

Hedden, T., Gabrieli, J.D.E., 2004. Insights into the ageing mind–A view from cognitive neuroscience. Nat. Rev. Neurosci. 5, 87–96.

Hipp, JF, Hawellek, DJ, Corbetta, M, Siegel, M, Engel, AK, 2012 Jun. Large-scale cortical correlation structure of spontaneous oscillatory activity. Nat Neurosci 15 (6), 884–890. doi:10.1038/nn.3101.

Hsu, D., Marshall, G.A., 2017. Primary and secondary prevention trials in Alzheimer's disease–Looking back, moving forward. Curr. Alzheimer's Res. 14, 426–440.

Ibrahim, B., Suppiah, S., Ibrahim, N., Mohamad, M., Hassan, H.A., Nasser, N.S., Saripan, M.I., 2021. Diagnostic power of resting-state fMRI for detection of network connectivity in Alzheimer's disease and mild cognitive impairment–A systematic review. Hum. Brain Mapp. 42, 2941–2968.

Ittner, L.M., Götz, J., 2011. Amyloid-β and tau–A toxic pas de deux in Alzheimer's disease. Nat. Rev. Neurosci. 12, 67–72.

Jockwitz, C., Caspers, S., Lux, S., Eickhoff, S.B., Jutten, K., Lenzen, S., Moebus, S., Pundt, N., Reid, A., Hoffstaedter, F., Jockel, K.H., Erbel, R., Cichon, S., Nothen, M.M., Shah, N.J., Zilles, K., Amunts, K., 2017. Influence of age and cognitive performance on resting-state brain networks of older adults in a population-based cohort. Cortex 89, 28–44.

Jones, D.T., Knopman, D.S., Gunter, J.L., Graff-Radford, J., Vemuri, P., Boeve, B.F., Petersen, R.C., Weiner, M.W., Jack Jr., C.R., 2016. Cascading network failure across the Alzheimer's disease spectrum. Brain 139, 547–562.

Jones, D.T., Machulda, M.M., Vemuri, P., McDade, E.M., Zeng, G., Senjem, M.L., Gunter, J.L., Przybelski, S.A., Avula, R.T., Knopman, D.S., Boeve, B.F., Petersen, R.C., Jack Jr., C.R., 2011. Age-related changes in the default mode network are more advanced in Alzheimer's disease. Neurology 77, 1524–1531.

Karran, E., Mercken, M., Strooper, B.D., 2011. The amyloid cascade hypothesis for Alzheimer's disease–An appraisal for the development of therapeutics. Nat. Rev. Drug Discov. 10, 698–712.

Lehmann, D., Ozaki, H., Pal, I., 1987. EEG alpha map series–Brain micro-states by space-oriented adaptive segmentation. Electroencephalogr. Clin. Neurophysiol. 67, 271–288.

Li, C., Yuan, H., Shou, G., Cha, Y.-H., Sunderam, S., Besio, W., Ding, L., 2018. Cortical statistical correlation tomography of EEG resting state networks. Front. Neurosci. 12.

Liu, Q., Farahibozorg, S., Porcaro, C., Wenderoth, N., Mantini, D., 2017. Detecting large-scale networks in the human brain using high-density electroencephalography. Hum. Brain Mapp. 38, 4631–4643.

Liu, T.T., 2013. Neurovascular factors in resting-state functional MRI. Neuroimage 80, 339–348.

Logothetis, N.K., 2008. What we can do and what we cannot do with fMRI. Nature 453, 869–878.

Luo, L., Craik, F.I.M., 2008. Aging and memory–A cognitive approach. Can. J. Psychiatry 53, 346–353.

Madden, D.J., 1990. Adult age differences in attentional selectivity and capacity. Eur. J. Cogn. Psychol. 2, 229–252.

McDade, E., Llibre-Guerra, J.J., Holtzman, D.M., Morris, J.C., Bateman, R.J., 2021. The informed road map to prevention of Alzheimer's Disease–A call to arms. Mol. Neurodegeneration 16, 49.

Mesulam, M.M., 1990. Large-scale neurocognitive networks and distributed processing for attention, language, and memory. Ann. Neurol. 28, 597–613.

Mevel, K., Chételat, G., Eustache, F., Desgranges, B., 2011. The default mode network in healthy aging and Alzheimer's disease. Int. J. Alzheimer's Dis. 2011, 535816.

Mormino, E.C., Smiljic, A., Hayenga, A.O., Onami, S.H., Greicius, M.D., Rabinovici, G.D., Janabi, M., Baker, S.L., Yen, I.V., Madison, C.M., Miller, B.L., Jagust, W.J., 2011. Relationships between β-amyloid and functional connectivity in different components of the default mode network in aging. Cereb. Cortex 21, 2399–2407.

Natu, V.S., Lin, J.-J., Burks, A., Arora, A., Rugg, M.D., Lega, B., 2019. Stimulation of the posterior cingulate cortex impairs episodic memory encoding. J. Neurosci. 39, 7173.

Newton, A.T., Morgan, V.L., Rogers, B.P., Gore, J.C., 2011. Modulation of steady state functional connectivity in the default mode and working memory networks by cognitive load. Hum. Brain Mapp. 32, 1649–1659.

Nunez, Paul L., Ramesh, Srinivasan., 2006. *Electric fields of the brain: the neurophysics of EEG*. Oxford University Press, USA.

O'Keeffe, J., Carlson, B., DeStefano, L., Wenger, M., Craft, M., Hershey, L., Hughes, J., Wu, D., Ding, L., Yuan, H., 2017. EEG fluctuations of wake and sleep in mild cognitive impairment. Conf. Proc. IEEE Eng. Med. Biol. Soc. 2017, 3612–3615.

de Pasquale, F, Della Penna, S, Snyder, AZ, Lewis, C, Mantini, D, Marzetti, L, Belardinelli, P, Ciancetta, L, Pizzella, V, Romani, GL, Corbetta, M, 2010 Mar 30. Temporal dynamics of spontaneous MEG activity in brain networks. Proc Natl Acad Sci U S A 107 (13), 6040–6045. doi:10.1073/pnas.0913863107.

Peters, R., 2006. Ageing and the brain. Postgrad. Med. J. 82, 84–88.

Petrella, J.R., Sheldon, F.C., Prince, S.E., Calhoun, V.D., Doraiswamy, P.M., 2011. Default mode network connectivity in stable vs progressive mild cognitive impairment. Neurology 76, 511–517.

Porsteinsson, A.P., Isaacson, R.S., Knox, S., Sabbagh, M.N., Rubino, I., 2021. Diagnosis of Early Alzheimer's Disease–Clinical Practice in 2021. J. Prev. Alzheimer's Dis. 8, 371–386.

Qi, Z., Wu, X., Wang, Z., Zhang, N., Dong, H., Yao, L., Li, K., 2010. Impairment and compensation coexist in amnestic MCI default mode network. Neuroimage 50, 48–55.

Rabin, L.A., Paré, N., Saykin, A.J., Brown, M.J., Wishart, H.A., Flashman, L.A., Santulli, R.B., 2009. Differential memory test sensitivity for diagnosing amnestic mild cognitive impairment and predicting conversion to Alzheimer's disease. Neuropsychol. Dev. Cogn. B Aging Neuropsychol. Cogn. 16, 357–376.

Race, E., Keane, M.M., Verfaellie, M., 2011. Medial temporal lobe damage causes deficits in episodic memory and episodic future thinking not attributable to deficits in narrative construction. J. Neurosci. 31, 10262–10269.

Raz, N., Rodrigue, K.M., 2006. Differential aging of the brain–Patterns, cognitive correlates and modifiers. Neurosci. Biobehav. Rev. 30, 730–748.

Royall, D.R., Chiodo, L.K., Polk, M.J., 2000. Correlates of disability among elderly retirees with "subclinical" cognitive impairment. J. Gerontol. A 55, M541–M546.

Royall, D.R., Cordes, J.A., Polk, M., 1998. CLOX–An executive clock drawing task. J. Neurol. Neurosurg. Psychiatry 64, 588–594.

Sambataro, F., Murty, V.P., Callicott, J.H., Tan, H.Y., Das, S., Weinberger, D.R., Mattay, V.S., 2010. Age-related alterations in default mode network–Impact on working memory performance. Neurobiol. Aging 31, 839–852.

Sestieri, C., Corbetta, M., Romani, G.L., Shulman, G.L., 2011. Episodic memory retrieval, parietal cortex, and the default mode network–Functional and topographic analyses. J. Neurosci. 31, 4407–4420.

Sheline, Y.I., Raichle, M.E., 2013. Resting state functional connectivity in preclinical Alzheimer's disease. Biol. Psychiatry 74, 340–347.

Sintini, I., Graff-Radford, J., Jones, D.T., Botha, H., Martin, P.R., Machulda, M.M., Schwarz, C.G., Senjem, M.L., Gunter, J.L., Jack, C.R., Lowe, V.J., Josephs, K.A., Whitwell, J.L., 2021. Tau and Amyloid relationships with resting-state functional connectivity in a typical Alzheimer's disease. Cereb. Cortex 31, 1693–1706.

Smith, A., 1982. Symbol Digit Modalities Test. Western Psychological Services, Los Angeles, CA.

Sorg, C., Riedl, V., Muhlau, M., Calhoun, V.D., Eichele, T., Laer, L., Drzezga, A., Forstl, H., Kurz, A., Zimmer, C., Wohlschlager, A.M., 2007. Selective changes of resting-state networks in individuals at risk for Alzheimer's disease. Proc. Natl. Acad. Sci. U. S. A. 104, 18760–18765.

Sperling, R., 2011. Potential of functional MRI as a biomarker in early Alzheimer's disease. Neurobiol. Aging 32 (Suppl 1), S37–S43.

Sperling, R., Mormino, E., Johnson, K., 2014. The evolution of preclinical Alzheimer's disease–Implications for prevention trials. Neuron 84, 608–622.

Sperling, R.A., Aisen, P.S., Beckett, L.A., Bennett, D.A., Craft, S., Fagan, A.M., Iwatsubo, T., Jack Jr., C.R., Kaye, J., Montine, T.J., Park, D.C., Reiman, E.M., Rowe, C.C., Siemers, E., Stern, Y., Yaffe, K., Carrillo, M.C., Thies, B., Morrison-Bogorad, M., Wagster, M.V., Phelps, C.H., 2011. Toward defining the preclinical stages of Alzheimer's disease–Recommendations from the National Institute on Aging-Alzheimer's Association workgroups on diagnostic guidelines for Alzheimer's disease. Alzheimers Dement. 7, 280–292.

Stroop, J.R., 1935. Studies of interference in serial verbal reactions. J. Exp. Psychol. 18, 643–662.

Sweeney, M.D., Kisler, K., Montagne, A., Toga, A.W., Zlokovic, B.V., 2018. The role of brain vasculature in neurodegenerative disorders. Nat. Neurosci. 21, 1318–1331.

Tromp, D., Dufour, A., Lithfous, S., Pebayle, T., Després, O., 2015. Episodic memory in normal aging and Alzheimer's disease–Insights from imaging and behavioral studies. Ageing Res. Rev. 24, 232–262.

Uttl, B., 2002. North American adult reading test–Age norms, reliability, and validity. J. Clin. Exp. Neuropsychol. 24, 1123–1137.

Van Dijk, K.R., Hedden, T., Venkataraman, A., Evans, K.C., Lazar, S.W., Buckner, R.L., 2010. Intrinsic functional connectivity as a tool for human connectomics–Theory, properties, and optimization. J. Neurophysiol. 103, 297–321.

Verhaeghen, P., Marcoen, A., Goossens, L., 1993. Facts and fiction about memory aging–A quantitative integration of research findings. J. Gerontol. 48, P157–P171.

Wang, K., Liang, M., Wang, L., Tian, L., Zhang, X., Li, K., Jiang, T., 2007. Altered functional connectivity in early Alzheimer's disease–A resting-state fMRI study. Hum. Brain Mapp. 28, 967–978.

Wang, L., Laviolette, P., O'Keefe, K., Putcha, D., Bakkour, A., Van Dijk, K.R., Pihlajamäki, M., Dickerson, B.C., Sperling, R.A., 2010. Intrinsic connectivity between the hippocampus and posteromedial cortex predicts memory performance in cognitively intact older individuals. Neuroimage 51, 910–917.

Wechsler, D., 1987. Manual for the Wechsler memory Scale-Revised. Psychological Corporation, San Antonio, TX.

Wenger, M.K., Negash, S., Petersen, R.C., Petersen, L., 2010. Modeling and estimating recall processing capacity–Sensitivity and diagnostic utility in application to mild cognitive impairment. J. Math. Psychol. 54, 73–89.

Whalley, L.J., Fox, H.C., Wahle, K.W., Starr, J.M., Deary, I.J., 2004. Cognitive aging, childhood intelligence, and the use of food supplements–Possible involvement of n−3 fatty acids. Am. J. Clin. Nutr. 80, 1650–1657.

Yeo, B.T., Krienen, F.M., Sepulcre, J., Sabuncu, M.R., Lashkari, D., Hollinshead, M., Roffman, J.L., Smoller, J.W., Zollei, L., Polimeni, J.R., Fischl, B., Liu, H., Buckner, R.L., 2011. The organization of the human cerebral cortex estimated by intrinsic functional connectivity. J. Neurophysiol. 106, 1125–1165.

Yu, M., Sporns, O., Saykin, A.J., 2021. The human connectome in Alzheimer's disease - relationship to biomarkers and genetics. Nat. Rev. Neurol. 17, 545–563.

Yuan, H., Ding, L., Zhu, M., Zotev, V., Phillips, R., Bodurka, J., 2016. Reconstructing large-scale brain resting-state networks from high-resolution EEG–Spatial and temporal comparisons with fMRI. Brain Connect. 6, 122–135.

Yuan, H., Phillips, R., Wong, C.K., Zotev, V., Misaki, M., Wurfel, B., Krueger, F., Feldner, M., Bodurka, J., 2018. Tracking resting state connectivity dynamics in veterans with PTSD. Neuroimage Clin. 19, 260–270.

Yuan, H., Young, K.D., Phillips, R., Zotev, V., Misaki, M., Bodurka, J., 2014. Resting-state functional connectivity modulation and sustained changes after real-time functional magnetic resonance imaging neurofeedback training in depression. Brain connect. 4, 690–701.

Yuan, H., Zotev, V., Phillips, R., Bodurka, J., 2013. Correlated slow fluctuations in respiration, EEG, and BOLD fMRI. Neuroimage 79, 81–93.

Yuan, H., Zotev, V., Phillips, R., Drevets, W.C., Bodurka, J., 2012. Spatiotemporal dynamics of the brain at rest–exploring EEG microstates as electrophysiological signatures of BOLD resting state networks. Neuroimage 60, 2062–2072.

Zhang, H.Y., Wang, S.J., Xing, J., Liu, B., Ma, Z.L., Yang, M., Zhang, Z.J., Teng, G.J., 2009. Detection of PCC functional connectivity characteristics in resting-state fMRI in mild Alzheimer's disease. Behav. Brain Res. 197, 103–108.

Zhang, Y., van Drongelen, W., He, B., 2006. Estimation of in vivo brain-to-skull conductivity ratio in humans. Appl. Phys. Lett. 89, 223903–2239033.

Zonneveld, H.I., Pruim, R.H., Bos, D., Vrooman, H.A., Muetzel, R.L., Hofman, A., Rombouts, S.A., van der Lugt, A., Niessen, W.J., Ikram, M.A., 2019. Patterns of functional connectivity in an aging population–The Rotterdam Study. Neuroimage 189, 432–444.